Eur Biophys J (2003) 32: 676–683
DOI 10.1007/s00249-003-0335-6

ARTICLE

Sean Sun · David Chandler · Aaron R. Dinner
George Oster

Elastic energy storage in β-sheets with application to F_1-ATPase

Received: 26 December 2002 / Revised: 11 March 2003 / Accepted: 4 April 2003 / Published online: 3 September 2003

Abstract We present a methodology for obtaining the elastic properties of protein motifs. We combine the use of interpolated structures (IS), molecular dynamics (MD) and collective coordinates to deduce the elastic properties of the β-sheet in F_1 ATPase. We find that about 3.5 kcal/mol (6 k_BT at room temperature) of elastic energy is stored in the β-sheet as the β-subunit undergoes its hinge bending motion, in good agreement with the finite element model of Wang and Oster [Nature (1998) 396:279–282]. The technique should be useful for β-sheets in other proteins and aid in the construction of phenomenological models for molecular motors that are computationally prohibitive for MD alone.

Introduction

Most protein motors are too large to be simulated, unbiased, by molecular dynamics in the near future. Molecular dynamics can be used together with more coarse-grained models to gain insight into long time scale processes. Slow conformational motions can be modeled as finite element elastic bodies whose motions are driven by chemically derived forces. The model of F_1 ATPase by Wang and Oster (1998) and Oster and Wang (2000a) is an example of this approach that has been successful in predicting the mechanical behavior of the motor. However, the elastic moduli of the constituent parts were free parameters used to fit the data. Models of this sort would benefit from a technique to estimate the overall elastic moduli of proteins from more fundamental considerations. We present here one such technique. We use as our test case the β-sheet of F_1 ATPase during its hydrolysis cycle.

We base our approach on combining four techniques. First, we deduce a set of collective coordinates to characterize the conformations of protein subunits as they undergo their cycle of deformations. Second, we employ a sequence of interpolated structures deduced from the atomic coordinates of the protein in two states along the hydrolysis reaction pathway to give an approximate picture of the conformational trajectory (Wang and Oster 1998). Third, we use molecular dynamics (MD) to refine these conformational snapshots by equilibrating each interpolated structure. Finally, we use umbrella sampling to deduce the relative free energies of each equilibrated structure. This allows us to determine the free energy changes along the collective coordinate, and from this to compute an overall effective elastic modulus of the β-sheet. This can be compared with the empirical value used by Wang and Oster to fit the mechanical measurements on the F_1 motor.

In order to develop the technique, we focus on the β-sheet itself and do not including the surrounding protein residues. Thus our estimate of the elastic modulus is not of the complete β-subunit. Nevertheless, we find that the value we compute for the elastic modulus is in reasonable agreement with the value used by Wang and Oster to fit the data. Examining the structure and the conformational change suggested by the interpolated structures suggests that the β-sheet is the major contributor to the overall elasticity, although a definitive answer requires a much more elaborate simulation of the complete system.

To the extent that our approach is useful, the overall elasticity of proteins should be decomposable into contributions from extended structural motifs such as β-sheets, which are ubiquitous in other molecular motors. Thus the technique presented here should be useful

S. Sun · G. Oster (✉)
Department of Molecular and Cellular Biology,
University of California, Berkeley, CA 94720, USA
E-mail: goster@nature.berkeley.edu

D. Chandler · A. R. Dinner
Department of Chemistry,
University of California, Berkeley, CA 94720, USA

in elucidating β-sheet contributions to elastic deformations in other motor proteins.

F_1-ATPase structure and conformational dynamics

Excellent summaries of the structure and function of ATP synthase can be found elsewhere (Pedersen 2000; Walker 2000). In brief, the F_1-ATPase is a hexameric ring of three alternating α- and β-subunits surrounding a central coiled-coil γ-shaft. Three catalytic sites are located at alternating interfaces between the α- and β-subunits. Nucleotide binding and hydrolysis result in large conformational changes in the β-subunit that drive rotation of the γ-subunit; the α-subunit is relatively rigid. Two different interpolation schemes between the ATP bound and the empty conformations of the β-subunit indicate that the principal motion of its two domains is a hinge bending movement (Wang and Oster 1998; Oster and Wang 2000a; Gerstein et al. 1994; Gerstein 1996). The angle between domains closes by about 30° in the ATP bound state when compared with the empty state. The interpolated structures served as the basis for a phenomenological model in which the β-subunit was treated as a hinge in parallel with an elastic spring that tends to restore the open configuration (Wang and Oster 1998; Oster and Wang 2000a). In this model, nucleotide binding drives the hinge-bending motion of the β-subunits, and this motion turns the γ-subunit by pushing on its off-axis eccentric portion. Good agreement with most of the experimentally observed kinetic and thermodynamic data was obtained using a value for the elastic spring constant of 4 pN/nm, corresponding to a deformation energy of 6 kcal/mol or about 10 k_BT at room temperature (Wang and Oster 1998; Oster and Wang 2000a).

Methods: umbrella sampling

Here, we describe the atomistic umbrella sampling simulations used to estimate the free energy of deformation of the β-sheet (Frenkel and Smit 1996; Torrie and Valleau 1974). We modeled the β-sheet (the residues detailed in the text) in vacuum (constant dielectric $\epsilon = 1$) with the CHARMM all-hydrogen parameter set released with version c22 (MacKerell et al. 1998; Brooks et al. 1983). There are no histidines in the β-sheet, and other titratable residues were assigned their standard protonation states at neutral pH. We use a nonbond cutoff distance of 14 Å.

We performed a total of 25 simulations. Each simulation corresponded to a different umbrella sampling window around one of the interpolated structures. For the i-th window, we added to the energy function a biasing potential of the form

$$V_I(G, M^2) = \frac{1}{2}k[(G(\mathbf{q}) - G_I)^2 + (M^2(\mathbf{q}) - M_I^2)^2] \quad (1)$$

where M_I^2 and G_I are the mean squared and Gaussian curvatures of interpolated structure I, $M^2(\mathbf{q})$ and $G(\mathbf{q})$ are the corresponding quantities fitted from atomic positions ($\mathbf{q}$) of the 35 nitrogens. k is a force constant. For all the windows, $k = 5.2\times10^{-7}$ kcal Å^4. This gives fluctuation of G and M^2 around 5×10^{-4} Å^{-2} so that the centers of the windows (G_I, M_I^2) are within the overlapping region.

To prevent the β-sheet from moving in space, we add a harmonic restraint to hold the C_α atoms of one of the outermost strands of the β-sheet (residues 216–220) close to their positions in the first interpolated structure. A relatively stiff force constant of 48 kcal mol^{-1} Å^{-2} was used. This energy term does not make a significant contribution to the free energy of deformation because most of the curvature changes are due to deformation at the other end of the sheet. The constraint energies calculated separately for each simulation window, varies by less than 1 k_BT.

The configuration space is sampled with Langevin dynamics in the CHARMM program (version c27b3) (Brooks). A friction constant of 10 ps^{-1} is applied to all the atoms (including the hydrogens), and the timestep is 1 fs. The SHAKE algorithm was used to constrain the lengths of bonds to hydrogen atoms (van Gunsteren and Berendsen 1977). The starting structure for each simulation was generated by minimizing the conformation of the β-sheet in the first interpolated structure (index $I = 0$) subject to the umbrella potential. This structure was heated from 100 K to 298 K over the course of 400 ps, and was then equilibrated for 1 ns. Equilibration at 298 K is checked by monitoring the average and fluctuation of the potential energy. Statistics are collected every 25 steps for 3 ns. For each MD step, $M^2(\mathbf{q})$ and $G(\mathbf{q})$ in Eq. (1) are calculated by fitting a new surface at every step of the molecular dynamics simulation. The corresponding forces from the umbrella potentials on the nitrogens are calculated using finite difference.

The probability of observing curvatures M^2 and G is given by collecting histograms for each biasing potential:

$$P_I(G, M^2) = \langle \delta(G - G(\mathbf{q}))\delta(M^2 - M^2(\mathbf{q}))\rangle_I \quad (2)$$

Here, the average runs over the saved configurations in simulation i and $\mathbf{q}$ is the vector describing the coordinates of the backbone nitrogen atoms at saved configurations. The bin size for the histograms is 2.07×10^{-4} Å^{-2}. The weighted histogram method (WHAM) (Kumar et al. 1992) is used to remove the bias due to the umbrella potential and contributions from multiple simulations are included appropriately to find the final unbiased histogram.

Results

Describing the elastic properties of the β-sheet

In order to describe the elastic property of the β-sheet in F_1, we identify the order parameters that we use to characterize the conformational changes associated with its deformation. As described earlier, the α-subunit is relatively rigid, and the β-subunit undergoes a hinge-bending motion of about 30° whose center is located near the β-sheet directly behind the ATP binding pocket. Figure 1 shows the spatial relationship between the ATP binding pocket and the β-sheet. The highlighted binding loops emanating from the β-sheet make direct contacts with the nucleotide during binding. To form all the necessary hydrogen-bonds when the nucleotide is tightly bound, the upper and lower loops must come together to enclose the nucleotide completely. Thus, as ATP binds to the catalytic site, it gradually forms the network of hydrogen-bonds within the binding pocket and stress is directly transmitted to the β-sheet. The formation and breaking of these hydrogen bonds is described in the companion paper (Antes et al. 2003).

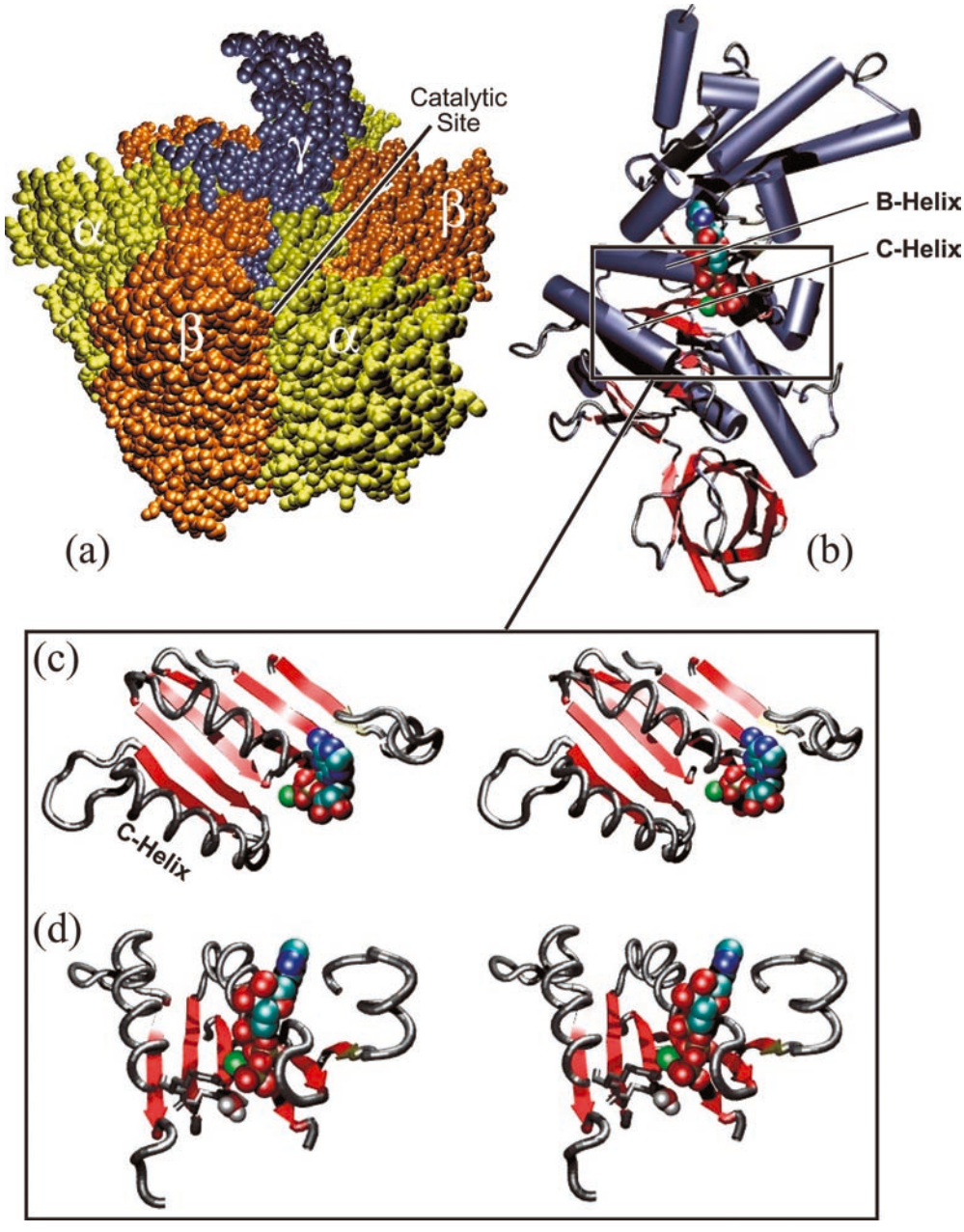

Fig. 1 a The F_1 portion of ATP synthase. **b** A β-subunit of F_1-ATPase showing the β-sheet and the loops containing the ATP binding residues. The ATP molecule is shown in space-filling mode viewed from the nucleotide end. Insets show stereo views. A ribbon diagram of the structure is given in the Supplemental Material. **c** The connectivity between the β-sheet and the three ATP binding loops (closed conformation). The left hand loop (C loop containing the C helix) contains the catalytic residue that holds the activated water for in-line attack on the γ-phosphate. It makes hydrogen bonds with the α and β phosphate oxygens. The P-loop containing the B helix makes hydrogen bonds with the oxygens of the γ-phosphate. The B loop makes hydrophobic contacts with the sugar end of the nucleotide. As ATP binds, the loops are pulled closer together, closing the binding pocket around the nucleotide. **d** A side view of the ATP binding pocket (closed conformation), showing the side-chains from loop B contacting the γ-phosphate. The water molecule that is involved in hydrolysis is also shown. A movie showing the complete conformational cycle is given in the Supplemental Material

As ATP settles into the pocket, the β-sheet undergoes a bend and a twist. Surrounding structural elements in the β-subunit remain almost undeformed throughout the motion, except for translations and rotations that do not change their shape. A reasonable conclusion from these observations is that part of the binding energy derived from ATP is stored in the elastic deformation of the β-sheet, while the balance is delivered to the γ-shaft. Thus, this β-sheet is the likely candidate for the elastic spring in the model of Wang and Oster (Wang and Oster 1998; Oster and Wang 2000a), and we study its properties in isolation.

To identify collective variables to describe the β-sheet, we use the following procedure based on the interpolated structures. We use 25 such structures equally spaced between the ATP bound conformation (interpolation index $I=0$) and the empty state (interpolation index $I=24$). We take the positions of the nitrogen atoms involved in the interstrand hydrogen bonds and consider them as points on a surface. If every atom is required to be strictly on the surface, then the surface would be very rough. A more sensible criterion is to use the positions of the nitrogen atoms to fit a smooth surface in a least squares sense to each of the interpolated structures. Then, as the β-sheet bends, the fitted surfaces provide a continuous description of the β-sheet geometry. The remarkable result is that this procedure yields a pair of collective coordinates that describe the

shape change of the β-sheet to high accuracy over the entire range of deformation. The procedure for defining these collective coordinates is as follows.

The β-sheet consists of residues 148–157, 180–190, 215–220, 249–259, 301–311 and 330–336 from PDB structure 1BMF. Of these, 35 nitrogens in residues 151–155, 181-186, 216–220, 250–256, 303–310 and 331–334 participate in the interstrand hydrogen bond network. We place our coordinate system in $\mathbf{R}^3$ at the center of mass of the raw PDB coordinates in the ATP bound structure ($I=0$). This coordinate system differs from the PDB coordinate system by a translation of the center of mass and a rigid rotation whose rotation angles are to be determined. In this 'centered' frame, we define a collection of quadratic surfaces $z^I = h^I(x^I,\ y^I)$, one such surface for each interpolated structure $I=0,\ ...,\ 24$. Each of these surfaces has the functional form:

$$h^I(x,y) = a_0^I + a_1^I x + a_2^I x^2 + a_3^I y + a_4^I xy + a_5^I y^2, \quad I = 0,\ldots,24 \tag{3}$$

where the coefficients a^I_j, $j=1,...,5$, are fitting parameters. For each interpolated structure I, we denote the atomic positions of the 35 hydrogen bonding nitrogens by $(x^I{}_\alpha, y^I{}_\alpha, z^I{}_\alpha)$, $\alpha=1,\ ...,\ 35$. Using a least square procedure, we minimize the distance between $z^I{}_\alpha$ and h^I by minimizing the error function

$$\text{Error}^I = \sum_{\alpha=1}^{35} \left[z^I_\alpha - h^I\left(x^I_\alpha, y^I_\alpha\right)\right]^2 \tag{4}$$

The sum is only over nitrogens involved in the interstrand hydrogen bonds. The coefficients, a^I_j, and hence Error^I, depend on our choice of coordinate frame. The particular frame we use is the one that minimizes the error of the fit for the initial structure (interpolation index 0). Subsequent analyses all use this coordinate frame. This procedure yields a set of five coefficients for each of the 25 interpolated structures. We use these fitted surfaces to define order parameters as follows.

The functional form of the surface in Eq. (3) is a simple quadratic polynomial. Figure 2a shows this surface for index 0 and 24. It is remarkable that, throughout the range of motion, the β-sheet at every interpolated structure is fit closely by such a surface: the average distance per nitrogen atom away from the fitted surface is $\approx$ 0.15 Å. Figure 2b plots the fitting error as a function of the interpolation index. We note that the fit error does depend on the choice of the coordinate frame to some extent and no particular frame minimizes the error for all the interpolation structures. Nevertheless, for such a simple fitting function, these errors are acceptable throughout the motion of the β-sheet.

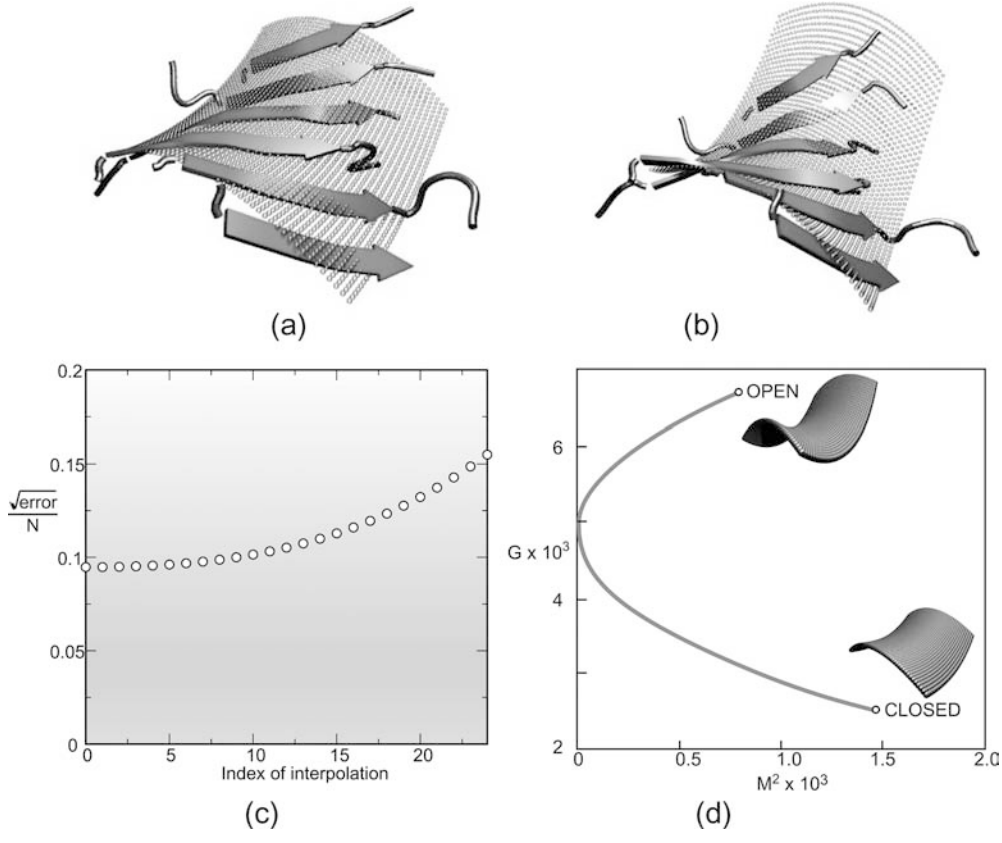

Fig. 2a–c Surface model of the β-sheet. **a** The open (left) and closed (right) conformation of the β-sheet. Also shown are the least square surface to the hydrogen-bonded nitrogens in the β-sheet. **b** The error per atom in fitting the quadratic surface to the β-sheet is less than 0.15Å. **c** The path in (G, M^2) coordinates representing the conformational change of the β-sheet according to the interpolated structures. Each interpolated structure and its associated surface gives a point on this path

The closeness of the quadratic fit to the interpolated structures of the β-sheet has an important consequence: the curvatures of these surfaces are *constant*. The mean (M) and Gaussian (G) curvatures of each surface can be computed from the trace and determinant, respectively, of the Hessian of $h^I(x, y)$ (O'Neill 1997):

$$M^I = \left[\left(\frac{\partial^2 h^I}{\partial x^2}\right) + \left(\frac{\partial^2 h^I}{\partial y^2}\right)\right] = 2(a_2^I + a_5^I)$$
$$G^I = \left[\left(\frac{\partial^2 h^I}{\partial x \partial y}\right)^2 - \left(\frac{\partial^2 h^I}{\partial x^2}\right)\cdot\left(\frac{\partial^2 h^I}{\partial y^2}\right)\right] = (a_4^I)^2 - 4a_2^I a_5^I \qquad (5)$$
$$I = 0,1,\ldots,24$$

Because the h^I are quadratic, M and G are constant for each interpolated structure. Thus, the bending and twisting motion of the β-sheet can be described by the mean and Gaussian curvature at each interpolated structure. For dimensional homogeneity, we choose as collective coordinates describing the β-sheet (M^2, G). Therefore, the interpolated structures correspond to a curve in (M^2, G) coordinates as shown in Fig. 2d, where points along this curve uniquely define the fitted surface. The elastic properties of the β-sheet as it undergoes the observed twist and bend can be computed from the free energy change as a function of M^2 and G, $F(M^2, G)$. The motivation for using mean and Gaussian curvature coordinates arises from the expression for the energy of an elastic plate (Landau and Lifshitz 1995).

The elastic energy stored in the β-sheet during bending

We can use the order parameters M^2 and G as the basis for umbrella sampling computations to estimate the free energy of deformation of the β-sheet. The bending of the β-subunit drives the power stroke of F_1, and this is tightly coupled to the deformation of the embedded β-sheet. Therefore, the free energy of deformation is directly related to the force generated by the motor. The total elastic energy of the β-subunit can be decomposed into three parts:

$$F(M^2, G) = \underbrace{F_s(M^2, G)}_{\beta-\text{sheet}} + \underbrace{F_p(M^2, G)}_{\text{Protein}} + \underbrace{\Delta F(M^2, G)}_{\text{Interaction}} \qquad (6)$$

where F_s is the bending free energy of the β-sheet, F_p is the free energy in the rest of the protein, and ΔF is the interaction free energy between the β-sheet and the surrounding protein. These quantities are all functions of the order parameters (M^2, G). Since the interpolated structures trace out the path shown in Fig. 2d, this path should be close to the path of minimum total free energy, $F(M^2,G)$. We calculate explicitly the free energy in the β-sheet, F_s, along the path defined in Fig. 2d. The contributions from the rest of the subunit will be important; however, it is not the focus of the present study.

The details of the MD simulation can be found in the Methods section. During the simulations, a fit to the quadratic surface of Eq. (3) is performed at each MD step, and statistics of M^2 and G are collected. The order parameters M^2 and G do not fully determine the microscopic configuration of the β-sheet, so that there exist configurations that require introducing higher order terms in Eq. (3) to yield fits with the same degrees of error. Conversely, there exist configurations that are fit well by the quadratic surface of Eq. (3) but are unlike structures typically observed in folded proteins. Any such configurations that yield similar values for the fitting parameters are in principle accessible in our simulations despite the umbrella potential added to restrain the system. Nevertheless, no such configurations are observed. The error of the fit to the constant curvature surfaces is not uniformly below 0.1 Å per nitrogen for every MD configuration. However, the largest fitting error is always below 0.25 Å per nitrogen, suggesting that their free energies are much higher than those of the interpolated conformations. This result provides further support for the idea that it is meaningful to model the shape of the β-sheet with a quadratic polynomial and view it as an elastic body. Although all possible configurations are accessible in spite of the umbrella potentials, no structures that are significantly different from the interpolated structures are observed. Therefore, it is reasonable to describe the β-sheet as an elastic surface by our procedure.

Results of the simulations are shown in Fig. 3 where the path suggested by the interpolated structure is shown as a dashed line. Several conclusions can be drawn from this data.

1. The path traced out by the interpolated structures is not a minimum energy path on the free energy surface; there are configurations away from the interpolated path that are more favorable. This is consistent with our earlier discussion of the total free energy versus the free energy of the individual parts. This suggests the surrounding material of the protein acts to restrict the accessible curvatures of the β-sheet.
2. Figure 4 shows the free energy along the curve traced by the interpolated structures. It decreases smoothly, and nearly linearly as the sheet deforms from the ATP bound closed structure ($I=0$) to the open configuration ($I=16$). This may contribute to the constant torque developed by the F_1 motor (Kinosita et al. 2000) as reflected in its high stokes efficiency (Oster and Wang 2000b; Wang and Oster 2001).
3. The open state of the β-subunit is the most energetically favorable configuration for the β-sheet. In multi-site hydrolysis, binding of ATP is coordinated with the release of ADP in the next site in the direction of rotation. Going from closed to open in Fig. 3, ADP release is assisted by the stored elastic energy in the β-sheet. However, force from the recoil of the

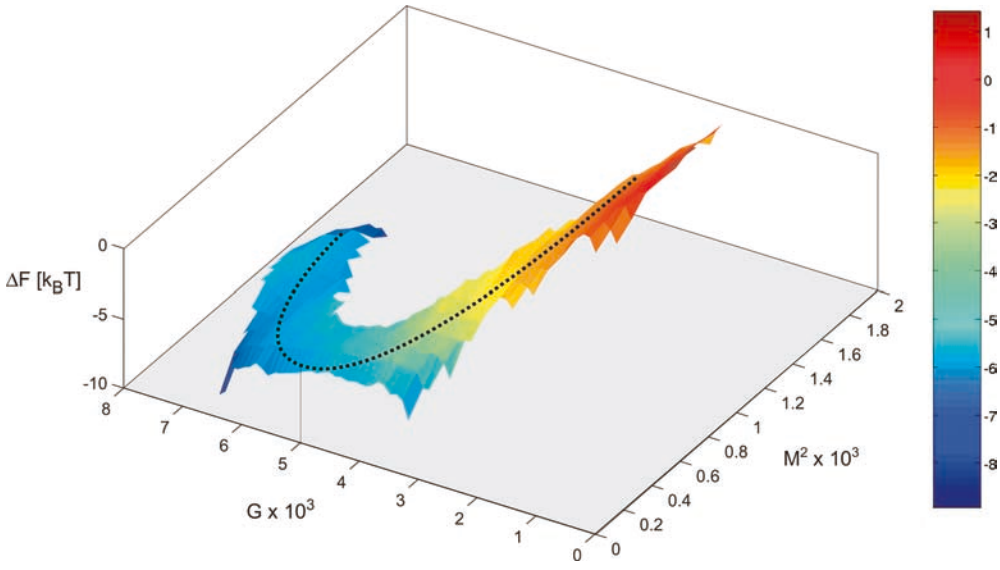

Fig. 3 The free energy surface, $F(G, M^2)$, of the β-sheet. The individual histograms are connected using weighted histogram method. The color scale shows the relative free energy. (*Red* is higher in free energy.) The *black* dotted line is the path in (G, M^2) space representing the interpolated structures shown in Fig. 1

β-sheet disappears around $I = 16$. Thus, product release may become more difficult towards the end of the power stroke.

4. The net free energy change between the closed and open configurations of the β-sheet is about 6 $k_B T$.
5. Most of the elastic energy is stored in bending, very little is stored in stretching of the sheet. During the simulation, the overall area of the β-sheet (calculated using triangulation with N-atoms as vertices of triangles) was monitored. For all the sampling windows, the area remained close to 405 Å^2 with a standard deviation less than 10 Å^2. Thus, the surface is not being stretched.

Discussion

Several molecular dynamics simulations on F_1 have appeared that study the dynamics that result from applying a rotational torque to the γ-shaft (Bockmann and Grubmuller 2002; Ma et al. 2002). However, the nanosecond time-scales of these simulations are still many decades away from the millisecond operating speed of this rotary motor; thus it is not clear how the driven configurations relate to the actual conformational pathway.

The interpolated structures suggest an alternative approach. Throughout the interpolation steps, no major violations of steric constraints are observed. Thus the interpolated structures offer a reasonable atomic scale picture of the protein's motion. Moreover, the interpolated structures paint a clear picture of how bending of the β-subunit leads to an overall rotation of the γ-shaft. Analysis of the interpolated structures show that the bending motion primarily distorts the parallel β-sheet directly behind the ATP binding pocket. The progressive formation of hydrogen bonds between the nucleotide and the catalytic pocket leads to a steady deformation of the β-sheet that stores elastic energy. When the hydrolysis products are released, the strain energy stored in the β-sheet should drive the recoil of the β-subunit to the open, unbent state. This recoil can play an important role in the mechanochemical cycle.

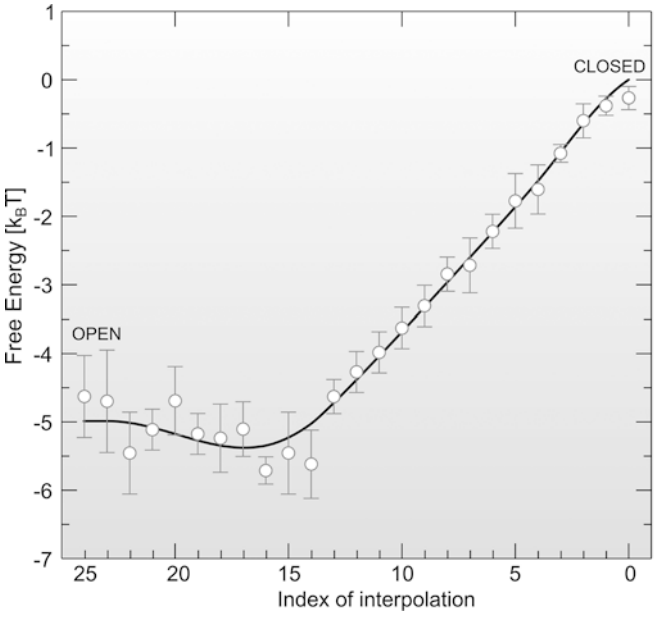

Fig. 4 Free energy of the β-sheet as it goes from closed to the open configuration along the interpolated path (symbols). This is simply an evaluation of $F(M^2,G)$ in Fig. 2d along the line. The open configuration is lower in energy by about 6 $k_B T$; i.e. as the system goes from open to closed, 6 $k_B T$ is stored as elastic strain energy. The solid curve is a polynomial fit to the symbols. The error bars are calculated using cumulative averages of the histograms

To investigate the mechanical properties of the β-sheet, we describe its interpolated conformations by fitting mathematical surfaces to the positions of the nitrogen atoms within the sheet. We find that surfaces of constant curvature approximate the observed conformations very well. Using atomistic molecular dynamics (MD) simulations and umbrella sampling, we find that the bare β-sheet in vacuum can store 3.5 kcal/mol (6 k_BT) of elastic energy as the β-subunit bends through its conformational trajectory. This free energy change during its deformation is consistent with the model calculations of Wang and Oster (Wang and Oster 1998; Oster and Wang 2000a). In those studies the conformational change of the β-subunit is modeled as a hinged spring. The spring constant necessary to match the experimental results is about 4 pN/nm which corresponds to a net free energy change of $\sim$10 k_BT. This value is in accord with biochemical studies on unisite kinetics, where the total free energy of hydrolysis is about 24 k_BT, of which 14 k_BT is associated with nucleotide binding and 10 k_BT with product release (Al-Shawi et al. 1989; Senior 1992). Wang and Oster ascribed the secondary free energy drop to elastic energy stored in the spring during ATP binding (Oster and Wang 2000a; Wang and Oster 1998). Our results here are consistent with that model if we view the β-sheet and its associated loops as the spring. Moreover, according to the 'binding zipper model' of Wang and Oster (Oster and Wang 2000a), the β-subunit bends as hydrogen bonds are formed progressively between the catalytic site and Mg^{++}·ATP (see Antes et al. 2003). Our simulations here indicate that the energy of hydrogen bond formation can be largely stored in the deformation induced in the β-sheet. When products are released after hydrolysis, the stored elastic energy in the β-sheet spring will help drive the recoil of the β subunit to the open configuration.

In addition to agreement with the theoretical models, biochemical studies (Iko et al. 2001) using mutants of F_1 show that torque generation can be enhanced or diminished by substituting residues in the β-sheet. These results support our conclusion that the β-sheet is an important elastic element in F_1. The precise effect of these mutations is unclear at the moment since non-native residues may change the local fold around the β-sheet. It is also clear that a complete understanding of torque generation in F_1 must take into account the remaining protein. The elastic property of the β-sheet composed with the rest of the protein is interesting for further investigation.

Protein structures can have interesting mechanical properties. Conformational changes of motor proteins occur in millisecond to microsecond regimes and involve collective motions of hundreds or thousands of atoms. In this study, we have shown how collective coordinates can describe the curvature of the β-sheet whose loops grasp the bound nucleotide. In terms of these collective coordinates, we showed that the bending and twisting of the β-sheet could act as a elastic hinge as the β-subunit bends. These collective coordinates are not linear combinations of atomic coordinates, and so elastic models based on normal modes cannot explain this motion. Since parallel β-sheets are ubiquitous in motor proteins, our study suggests that β-sheet deformation may play a role in the mechanical motions of other protein motors. The technique we have developed here may prove useful for describing the elastic properties of other protein motifs, such as coiled coils.

Acknowledgements GFO and SS were supported by NIH Grant GM59875–02. ARD was supported by a Burroughs Wellcome Fund Hitchings-Elion Fellowship. DC was supported by NSF Grant CHE-0078458. Computational resources were provided by an equipment grant from DOE Office of Basic Energy Sciences #DE-FG03–87ER13793. The authors thank H-Y Wang and Iris Antes for valuable discussions during the course of this work.

References

Al-Shawi M, Parsonage D, Senior A (1989) J Biol Chem 264:15376–15383

Antes I, Chandler D, Wang H, Oster G (2003) A molecular dynamics study of the unbinding of ATP from the catalytic site of F1-ATPase. Biophys J 82:2

Bockmann R, Grubmuller H (2002) Nanoseconds molecular dynamics simulation of primary mechanical energy transfer steps in F1-ATP synthase. Nature Struct Biol 9:198–202

Brooks B et al (1983) A program for macromolecular energy, minimization, and dynamics calculations. J Comput Chem 4:187–217

Frenkel D, Smit B (1996) Understanding Molecular Simulations. Academic Press, San Diego, Calif.

Gerstein M (1996) A protein motions database. In: Subbiah S (ed) Protein motions. Chapman and Hall, New York, pp 81–90

Gerstein M, Lesk A, Chothia C (1994) Structural mechanisms for domain movements in proteins. Biochemistry 33:6739–6749

Iko Y et al (2001) ATP synthase F1 sector rotation: defective torque generation in the β-subunit SER174 to PHE mutant and its suppression by second mutations. J Biol Chem 276:47508–47511

Kinosita K, Yasuda R, Noji H, Adachi K (2000) A rotary molecular motor that can work at near 100% efficiency. Philos Trans Biol Sci 355:473–490

Kumar S, Bouzida D, Swendsen R, Kollman P, Rosenberg J (1992) The weighted histogram analysis method for free-energy calculations on biomolecules. I. The method. J Comput Chem 13:1011–1021

Landau L, Lifshitz E (1995) The Theory of Elasticity. Butterworth-Heinemann, Boston, Mass.

Ma J et al (2002) A dynamic analysis of the rotation mechanism for conformational change in F1-ATPase. Structure 10:921–931

MacKerell A et al (1998) All-atom empirical potential for molecular modeling and dynamics. Studies of proteins. J Phys Chem B 102:3586–3616

O'Neill B (1997) Elementary differential geometry. Academic Press, San Diego, Calif., p 448

Oster G, Wang H (2000a) Reverse engineering a protein: The mechanochemistry of ATP synthase. Biochim Biophys Acta 1458:482–510

Oster G, Wang H (2000b) Why is the efficiency of the F1 ATPase so high? J Bioenerg Biomembr 332:459–469

Pedersen P (ed) (2000) ATP synthesis in the year 2000. Kluwer, New York, pp 423–546

Senior A (1992) J Bioenergetics Biomembranes 24:479–483
Torrie G, Valleau J (1974) Monte Carlo free energy estimates using non-Boltzmann sampling, application to the subcritical Lennard-Jones fluid. Chem Phys Lett 28:578–581
van Gunsteren W, Berendsen H (1977) Algorithms for macromolecular dynamics and constraint dynamics. Mol Phys 34:1311–1327
Walker J (ed) (2000) The mechanism of F_1 F_o-ATPase. Elsevier, New York, pp 221–514
Wang H, Oster G (1998) Energy transduction in the F1 motor of ATP synthase. Nature 396:279–282
Wang H, Oster G (2001) The Stokes efficiency for molecular motors and its applications. Europhys Lett 57:134–140